



Contents lists available at ScienceDirect

Biochemical and Biophysical Research Communications

journal homepage: www.elsevier.com/locate/ybbrc

Induction of ferroptosis by singlet oxygen generated from naphthalene endoperoxide

Takujiro Homma^{*}, Sho Kobayashi, Junichi Fujii

Department of Biochemistry and Molecular Biology, Graduate School of Medical Science, Yamagata University, 2-2-2 Iidanishi, Yamagata, 990-9585, Japan

ARTICLE INFO

Article history:

Received 10 August 2019

Accepted 13 August 2019

Available online xxx

Keywords:

Singlet oxygen

ferroptosis

Lipid peroxidation

ROS

Glutathione

ABSTRACT

Singlet oxygen causes a cytotoxic process in tumor cells in photodynamic therapy (PDT) and skin phototaging. The mechanism responsible for this cytotoxicity is, however, not fully understood. 1-Methylnaphthalene-4-propionate endoperoxide (MNPE) is a cell-permeable endoperoxide that generates pure singlet oxygen. We previously reported that cell death induced by MNPE did not show the typical profile of apoptosis, and the cause of this cell death remains elusive. We report herein on an investigation of the mechanism for MNPE-induced cell death from the view point of ferroptosis. The findings indicate that the MNPE treatment decreased the viabilities of mouse hepatoma Hepa 1-6 cells in vitro, and that this decrease was accompanied by increases in the concentrations of both intracellular ferrous iron and the level of lipid peroxidation, but that the caspase-mediated apoptotic pathway was not activated. The intracellular levels of cysteine and glutathione were not affected by the MNPE treatment. Importantly, an assay of lactate dehydrogenase activity revealed that the cell death caused by MNPE was suppressed by ferrostatin-1, a ferroptosis-specific inhibitor. Collectively, these results strongly indicate that ferroptosis is the main cell death pathway induced by singlet oxygen.

© 2019 Elsevier Inc. All rights reserved.

1. Introduction

Ferroptosis is a newly characterized type of non-apoptotic regulated cell death in which free iron and lipid peroxidation products are characteristically involved [1]. Ferroptosis appears to depend on ferrous iron, which can donate an electron to hydrogen peroxide, resulting in the formation of hydroxyl radicals by the Fenton reaction, which, in turn, react with polyunsaturated fatty acids to produce lipid peroxides. Because phospholipid hydroperoxide glutathione peroxidase (Gpx4) effectively suppresses ferroptosis, it is generally assumed that lipid peroxides function as the key driver of ferroptosis [2,3].

Singlet oxygen is not a radical but a highly reactive oxygen species (ROS) and is responsible for skin damage induced by UVA irradiation [4–6] and for the cytotoxic anti-cancer effect in photodynamic therapy (PDT) [7]. Despite its significant role in sunburn and PDT, the biological effects of singlet oxygen are not fully understood, and one of the reasons for this is that an appropriate system for producing pure singlet oxygen is essentially not

available. 1-Methylnaphthalene-4-propionate endoperoxide (MNPE) is a cell-permeable endoperoxide that generates pure singlet oxygen. Using MNPE, we previously reported that singlet oxygen is highly toxic and causes a non-apoptotic type of cell death [8–10]. Although this process is accompanied by the release of cytochrome *c* from mitochondria, cell death induced by MNPE does not show the typical profile of apoptosis, but instead appears to have necrosis-like characteristics [8]. This abortive apoptotic pathway is mainly due to the direct inhibition of caspase activity through protein modification by singlet oxygen [10]. Because proteases that contain catalytic cysteine (Cys) residues are highly sensitive to singlet oxygen-mediated inactivation [9,11], a reactive Cys at the catalytic center in caspases would also be susceptible to oxidative modification by singlet oxygen.

Although singlet oxygen is known to react with multiple cellular components, its preference for reacting with conjugated double bonds is very high, and hence it preferentially attacks polyunsaturated fatty acids in cells [12]. In fact lipid peroxides are involved in the cytotoxic action of singlet oxygen released from MNPE [8,9]. Treatment with vitamin E, a lipophilic antioxidant or the overexpression of Gpx4 protects cells against MNPE-induced cell death, while a hydrophilic antioxidant vitamin C fails to suppress the cell death.

^{*} Corresponding author.

E-mail address: tkhomma@med.id.yamagata-u.ac.jp (T. Homma).

Abbreviations

Cys	cysteine
GSH	glutathione
Gpx4	phospholipid hydroperoxide glutathione peroxidase
MNPE	1-methylnaphthalene-4-propionate endoperoxide
PDT	photodynamic therapy
ROS	reactive oxygen species
LC-MS	liquid chromatography-mass spectrometry

Based on these observations, we hypothesized that singlet oxygen causes ferroptosis by means of its ability to trigger lipid peroxidation. In the present study, we examined the issue of how singlet oxygen causes cell death by employing MNPE and the findings indicate that ferroptosis is actually the main cell death pathway that is induced by singlet oxygen.

2. Materials and methods**2.1. Cell culture and treatment**

Hepa 1-6 cells, a mouse hepatoma-derived cell line, were obtained from the RIKEN Bioresource Center (Tsukuba, Japan) and were utilized in this study as described in a previous report [13]. Briefly, the cells were maintained in Dulbecco's Modified Eagle's Medium (DMEM; FUJIFILM Wako Pure Chemical, Osaka, Japan; 044-29765) supplemented with 10% fetal bovine serum (FBS; Biowest, Riverside, MO, USA) and a penicillin-streptomycin solution (FUJIFILM Wako Pure Chemical) at 37 °C in a 5% CO₂ incubator. Where indicated, the cells were treated with dimethyl sulfoxide (DMSO; FUJIFILM Wako Pure Chemical) as a vehicle, 1-methylnaphthalene-4-propionate endoperoxide (MNPE; Waken B Tech., Ltd, Kyoto, Japan), ferrostatin-1 (Cayman Chemical, Ann Arbor, MI, USA), or staurosporine (FUJIFILM Wako Pure Chemical). For the MNPE treatment, Hepa 1-6 cells were initially treated with MNPE for 2 h, after which the media was exchanged for fresh media, and the preparation then incubated further until cell harvest, as previously described [8].

2.2. Evaluation of the viability and cytotoxicity of cells

Cells were seeded at an initial density of (1 × 10⁵/ml). Cell viability was determined using a CellTiter-Blue® Cell Viability Assay (Promega, Madison, WI, USA) according to the manufacturer's instructions. Fluorescence intensity was measured using a microplate reader Valioskan Flash (Thermo Fisher Scientific, Waltham, MA, USA) with an excitation wavelength of 560 nm and an emission wavelength of 590 nm. Cytotoxicity was determined by means of a lactate dehydrogenase (LDH) assay as described previously with minor modifications [8]. The reaction mixture contained 20 µl of the culture medium, 0.3 mM NADH, 1 mM sodium pyruvate, and 200 mM sodium phosphate buffer, pH 7.4 in total of 100 µl. Initial activities were calculated from the rate of disappearance of NADH during the starting linear phase of the reaction by monitoring the absorbance at 340 nm.

2.3. Western blotting

Cells were lysed in cold lysis buffer (50 mM Tris-HCl pH 7.5, 150 mM NaCl, 0.5% Triton X-100, 0.5% sodium deoxycholate, 2 mM

EDTA), supplemented with a protease inhibitor cocktail (Sigma-Aldrich, St. Louis, MO, USA; P8340). The lysate was centrifuged at 15,000×g for 10 min in a microcentrifuge. Protein concentrations were determined using a Pierce™ BCA Protein Assay Kit (Thermo Fisher Scientific). The proteins were separated on SDS-polyacrylamide gels and blotted onto polyvinylidene difluoride (PVDF) membranes (GE Healthcare, Chicago, IL, USA). The blots were then blocked with 5% skim milk in Tris-buffered saline containing 0.1% Tween-20 (TBST), and incubated overnight with the primary antibodies diluted in TBST. The primary antibodies used in the study were: Caspase-3 (R&D Systems, Minneapolis, MN, USA; AF-605-NA), cleaved caspase-3 (Cell Signaling Technology, Danvers, MA, USA; #9664), and GAPDH (Santa Cruz Biotechnology, Dallas, TX, USA; sc-25778). After three washings with TBST, the blots were incubated with horseradish peroxidase (HRP)-conjugated anti-goat (Santa Cruz Biotechnology; sc-2020) or anti-rabbit (Santa Cruz Biotechnology; sc-2004) secondary antibodies. After further washing, the bands were detected using the Immobilon western chemiluminescent HRP substrate (Merck Millipore, Burlington, MA, USA) on an image analyzer (ImageQuant LAS500, GE Healthcare).

2.4. Detection of fragmented DNA by agarose gel electrophoresis

DNA was isolated using a conventional procedure of phenol-chloroform extraction and isopropanol precipitation. The DNA samples were electrophoresed on a 1% agarose gel in Tris-acetate-EDTA buffer, then visualized on ImageQuant LAS500 after staining with 0.5 mg/ml ethidium bromide.

2.5. Liquid chromatography-mass spectrometry (LC-MS) analyses

LC-MS analyses of the intracellular contents of Cys and GSH were performed as described previously [13]. Briefly, the collected cells were homogenized in 200 µl of 50 mM ammonium bicarbonate, pH 8.0, containing 20 mM N-ethylmaleimide (NEM; FUJIFILM Wako Pure Chemical). A 50 µl aliquot of the sample was mixed with 100 µl of methanol containing 5 µM N-methylmaleimide (NMM)-derivatized GSH as an internal standard and an additional 100 µl of chloroform, the mixture was thoroughly stirred and centrifuged at 12,000×g for 15 min at 4 °C. The upper aqueous layer was filtered through 0.45 µm filters (Millex®-LH, Merck Millipore). A 90 µl aliquot of the filtrate was lyophilized, the residue dissolved in 30 µl of Milli-Q water, and then subjected to LC-MS analyses. A Q Exactive Hybrid Quadruple-Orbitrap mass spectrometer (Thermo Fisher Scientific) was operated in the positive ionization mode. The Ultimate 3000 liquid chromatography system consisted of a WPS-3000 TRS autosampler, a TCC-3000 RS column oven, and an HPG-3400RS quaternary pump (Dionex, Sunnyvale, CA). A SeQuant® ZIC®-pHILIC column (2.1 × 150 mm, 5 µm particle size; Merck KGaA, Germany) was maintained at 30 °C. Mobile phase A was 20 mM ammonium bicarbonate, pH 9.8, and mobile phase B was 100% acetonitrile. System control, data acquisition, and quantitative analysis were performed with the Xcalibur 2.2 software. Standard curves for GSH-NEM, and Cys-NEM showed linearity in the concentration ranges examined.

2.6. Flow cytometry

Cells were incubated with 10 µM C11-BODIPY 581/591 (Thermo Fisher Scientific) in the culture medium for 1 h and then washed with PBS. After trypsinization, the cells were collected and subjected to flow cytometry (FACSCanto™ II, BD Biosciences, Tokyo, Japan) at an excitation wavelength of 488 nm and an emission wavelength of 517–527 nm.

2.7. Detection of intracellular ferrous iron under fluorescent microscopy

Cells were incubated with 5 μM FeRhoNoxTM-1 (Goryo Chemical, Sapporo, Japan) according to the manufacturer's instructions. The cells were then washed with PBS and images were obtained using a BZ-X700 microscope (KEYENCE, Osaka, Japan).

2.8. Immunostaining

Cells were washed with PBS and fixed in 4% formaldehyde for 15 min at room temperature. After washing twice with PBS, the cells were permeabilized for 5 min with 0.5% Triton X-100 in PBS, then blocked for 30 min by treatment with 1% BSA in PBS at room temperature, and incubated overnight with anti-HNE (JaICA, Fukuroi, Japan, dilution 1:500) antibodies at 4 °C. After three washes in PBS, the cells were further incubated with a goat anti-mouse IgG (H + L), Alexa Fluor® 488 conjugate antibody (Thermo Fisher Scientific, dilution 1:500) for 60 min at room temperature. All images were obtained using a BZ-X700 microscope (KEYENCE).

2.9. Statistical analysis

Statistical analyses were performed using the GraphPad Prism 6

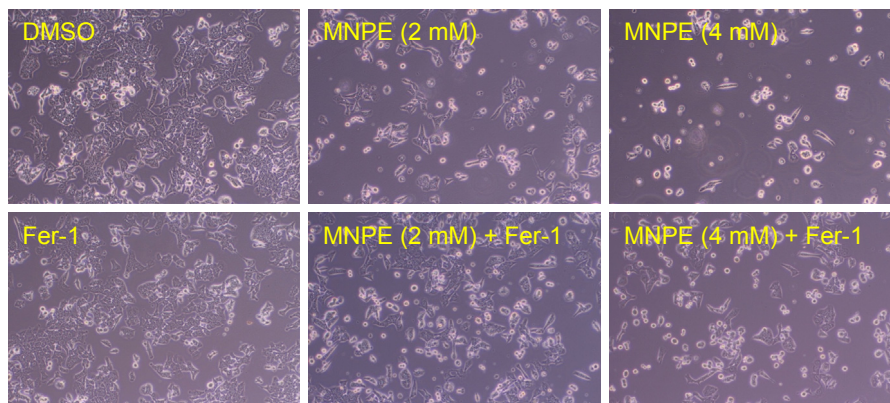
software (San Diego, CA, USA). A *P*-value of less than 0.05 was considered to be significant.

3. Results

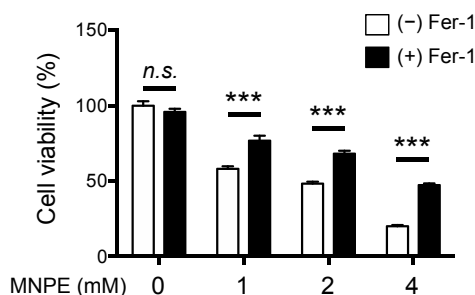
3.1. MNPE induces ferroptosis

Our objective was to investigate the cytotoxic effect of singlet oxygen released from MNPE in Hepa 1-6 cells in which ferroptosis had been previously implicated [13]. We examined MNPE-induced changes in the viabilities of Hepa 1-6 cells by using phase-contrast microscopy and CellTiter-Blue® Cell Viability Assays. Compared with DMSO-treated cells, the viabilities of the Hepa 1-6 cells were drastically decreased by MNPE in a dose-dependent manner (Fig. 1A and B). An assay for LDH release revealed that MNPE induced cell death during a 24 h period of incubation while MNP, a precursor of MNPE, had no effect on LDH release under these conditions, suggesting that the decreased viability of Hepa 1-6 cells was caused by cell death triggered by singlet oxygen generated from MNPE (Fig. 1C). Importantly, the lethal effects of MNPE were suppressed by ferrostatin-1, a ferroptosis-specific inhibitor that functions by preventing the accumulation of lipid peroxides [1], suggesting that MNPE-induced cell death is associated with ferroptosis.

A



B



C

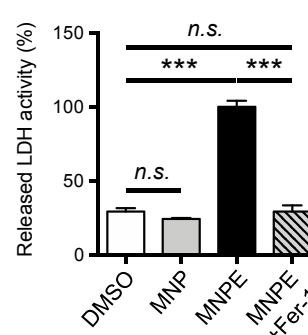


Fig. 1. MNPE induces ferroptotic cell death. (A) Representative phase-contrast images of cells after treatment with MNPE. Hepa 1-6 cells were treated with 2 or 4 mM MNPE for 2 h and then incubated in fresh medium for an additional 22 h in the presence or absence of 10 μM ferrostatin-1 (Fer-1). (B) Viability of cells was assessed by CellTiter-Blue® Cell Viability Assay. Hepa 1-6 cells were treated with indicated doses of MNPE for 2 h and then incubated in fresh medium for an additional 22 h in the presence or absence of 10 μM ferrostatin-1 (Fer-1). Data represent the mean \pm SEM ($n = 3$). *** $P < 0.001$ (Tukey's test). *n. s.*, not significant. (C) Cytotoxicity of cells was assessed by measuring released LDH activity. Hepa 1-6 cells were treated with 4 mM MNPE or MNP (a precursor of MNPE) for 2 h and then incubated in fresh medium for an additional 22 h in the presence or absence of 10 μM ferrostatin-1 (Fer-1). MNP was prepared by incubating MNPE at 37 °C for 3 h. Data represent the mean \pm SEM ($n = 3$). *** $P < 0.001$ (Tukey's test). *n. s.*, not significant. (For interpretation of the references to colour in this figure legend, the reader is referred to the Web version of this article.)

We then further characterized the cellular damage induced by MNPE treatment. DNA fragmentation, one of the representative criteria of apoptosis, was examined by examining DNA extracted from the cells that had been treated with MNPE or staurosporine, a well-known apoptotic inducer, on agarose gels. DNA fragmentation was observed only in the cells that had been treated with staurosporine, and not in the cells that had been treated with MNPE (Fig. 2A). Since DNA fragmentation and the subsequent apoptotic process are triggered by the activation of caspases, we analyzed the proteolytic activation of caspase 3, an executioner caspase of apoptosis. As we expected, the cleavage of procaspase 3 was observed only after treatment with staurosporine, but not in response to MNPE (Fig. 2B). These results indicate that MNPE is capable of inducing Hepa 1-6 cell death without activating caspases, consistent with previously reported findings [8].

3.2. MNPE induces lipid peroxidation

We next investigated the issue of whether MNPE causes lipid peroxidation, a hallmark of ferroptosis. After treating Hepa 1-6 cells with MNPE, the increase in fluorescence intensity of the lipid peroxidation probe C11-BODIPY was monitored by flow cytometry (Fig. 3A and B) and fluorescent microscopy (Fig. 3C). The MNPE-treated cells showed an increase in the fluorescence at 24 h after the treatment, and this increase was suppressed by a co-treatment with ferrostatin-1. We also examined the oxidation of intrinsic lipids in the MNPE-treated cells by determining the accumulation of 4-hydroxynonenal (4-HNE), a predominant lipid peroxidation product, using a specific antibody, by fluorescent microscopy (Fig. 3C). MNPE-treated cells showed a greater increase in 4-HNE adducts compared to the control cells. Co-treatment with ferrostatin-1 again significantly suppressed lipid peroxidation in the cells.

We also evaluated the intracellular levels of ferrous iron, another hallmark of ferroptosis, using the specific fluorescent probe FeRhoNox™-1 [14] under a fluorescent microscopy. The results showed that the MNPE treatment resulted in an increase in the fluorescent intensity of the cells, confirming an increase in the concentration of intracellular ferrous iron (Fig. 3D).

3.3. MNPE does not alter Cys-GSH status

Glutathione (GSH), a Cys-centered tripeptide, has pleiotropic functions in redox homeostasis, and the availability of Cys limits the extent of GSH synthesis under conditions of cell culture. Because cells with a GSH insufficiency are susceptible to ferroptotic cell death, we measured the intracellular levels of Cys and GSH in the cells that had been treated with MNPE. As a result, we found that they were not significantly affected by MNPE (Fig. 4A and B). It therefore appears that singlet oxygen released from MNPE induces ferroptosis without affecting Cys-GSH status.

4. Discussion

The findings reported herein indicate that an MNPE treatment induces cell death (Fig. 1), which had the following characteristics: a necrotic pattern with caspase-independency (Fig. 2) and increases in the levels of lipid peroxidation and ferrous iron (Fig. 3). This cell death and lipid peroxidation were rescued by ferrostatin-1. Based on these observations, it is conceivable that singlet oxygen released from MNPE caused ferroptosis in Hepa 1-6 cells. It is also noteworthy that the MNPE treatment did not affect the Cys-GSH status (Fig. 4), which, at first glance, appears to not be consistent with the original findings of ferroptosis [1] and many other cases of ferroptosis [15]. However, considering that singlet oxygen peroxidizes unsaturated fatty acids [12] and that lipid peroxides are direct mediators of ferroptosis [16], the ferroptotic pathway could be

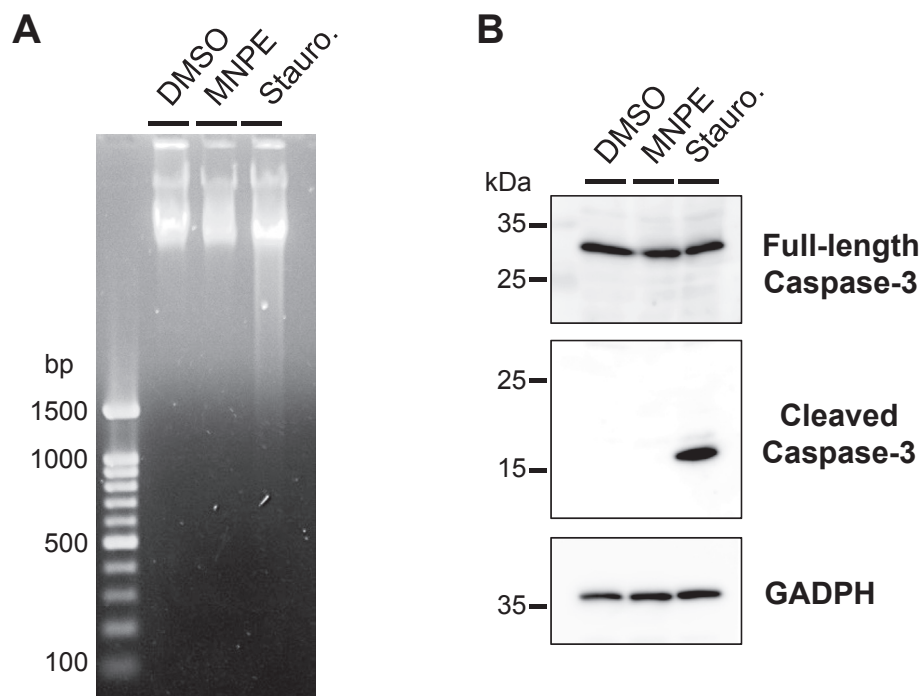


Fig. 2. Effects of MNPE on hallmarks of apoptosis. (A) Effect of MNPE on DNA ladder formation. Hepa 1-6 cells were treated with 4 mM MNPE for 2 h and then incubated in fresh medium for an additional 10 h. For a positive control, cells were treated with 1 μ M staurosporine (Stauro) for 12 h. DNA was extracted from the cells, separated on a 1% agarose gel and stained with ethidium bromide (B) Western blot analysis of caspase-3 in cells. Hepa 1-6 cells were treated under the same conditions as (A) and lysates were blotted for full length caspase-3, cleaved caspase-3, and GAPDH.

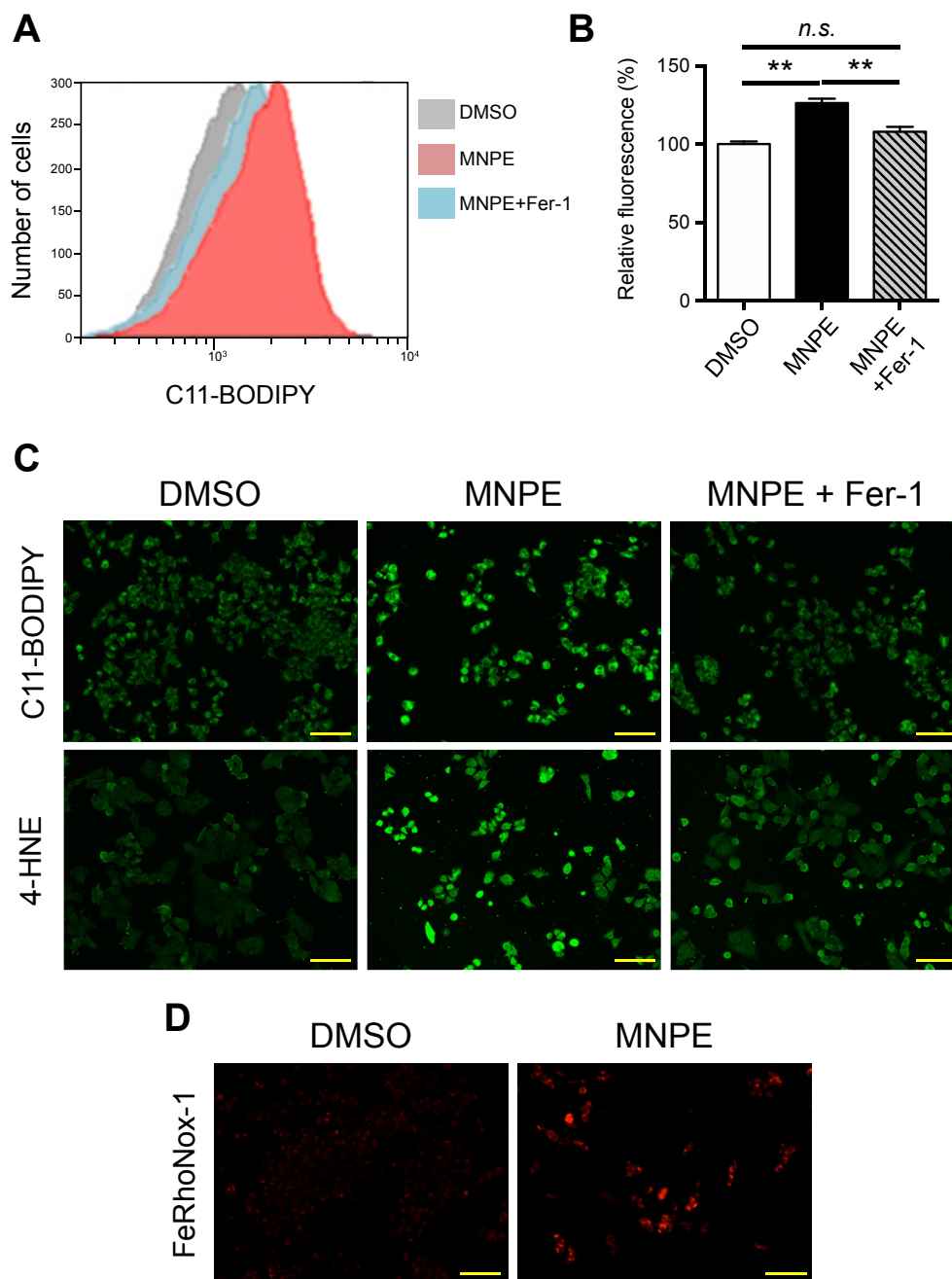


Fig. 3. Effects of MNPE on the hallmarks of ferroptosis. (A) Lipid ROS production assessed by flow cytometry using a C11-BODIPY 581/591. Hepa 1-6 cells were treated with 2 mM MNPE for 2 h and then incubated in fresh medium for an additional 22 h in the presence or absence of 10 μ M ferrostatin-1 (Fer-1). (B) Quantitative analysis of Lipid ROS levels from (A). Data are presented as the mean \pm SEM (n = 3). ** P < 0.01 (Tukey's test). n. s., not significant. (C) Hepa 1-6 cells were treated with 4 mM MNPE for 2 h and then incubated in fresh medium for an additional 22 h in the presence or absence of 10 μ M ferrostatin-1 (Fer-1), and then a C11-BODIPY and 4-HNE-adducts were visualized. Bars: 100 μ m. (D) Hepa 1-6 cells were treated with 4 mM MNPE for 2 h and then incubated in fresh medium for an additional 22 h, and intracellular ferrous iron was then visualized. Bars: 100 μ m.

activated by singlet oxygen during the process of lipid peroxidation, downstream of the Cys-GSH axis.

The MNPE treatment did not activate the caspase-mediated apoptotic pathway (Fig. 2) but induced ferroptosis (Figs. 1 and 3). We have consistently demonstrated that singlet oxygen released from MNPE actually inhibits the action of caspases and results in the abortion of the apoptotic process [8,10]. These findings may give an erroneous impression as compared with the previous reports showing that caspase activation during cell death is induced by singlet oxygen [17–20]. All of these studies involved the use of photosensitizers including rose bengal and methylene blue as

generators of singlet oxygen. Because not only singlet oxygen but also other ROS (including free radicals) are generated during photosensitization [7], different types of cell death may occur simultaneously under these experimental conditions. Compared to other ROS, the reactions of singlet oxygen with biological molecules are actually rather specific [12]. Therefore, caspase activation under these conditions may not represent the result of singlet oxygen, but the combined effects of ROS. Because MNPE generates “pure” singlet oxygen with no radical formation through thermal decomposition under physiological conditions [21–23], MNPE would be a reliable tool for investigating the specific function of singlet oxygen

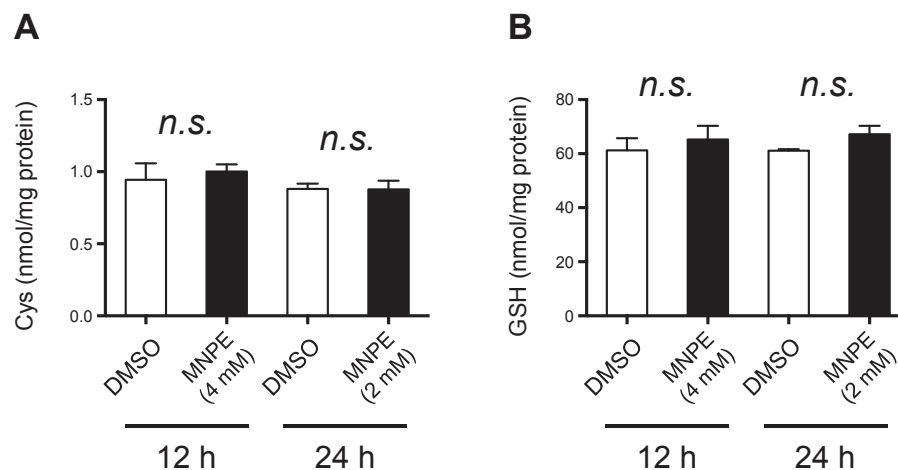


Fig. 4. Effects of MNPE on GSH levels during ferroptosis. Hepa 1-6 cells were treated with DMSO or MNPE at indicated conditions (first 2 h for treating) and then the intracellular contents of (A) Cys and (B) GSH were measured. Data are presented as the mean \pm SEM ($n = 3-4$). *n. s.*, not significant (Student's *t*-test).

in biological systems.

Having confirmed the fact that MNPE-derived singlet oxygen triggers ferroptosis, we directed our attention to the underlying mechanism for this process. For convenience, ferroptosis-inducing agents can be divided into two classes [15]; class 1 inducers decrease intracellular GSH (e.g. buthionine sulfoximine, erastin) and class 2 inducers directly inhibit Gpx4 through active site inhibition (e.g. RSL3). While the MNPE treatment had no effect on the Cys-GSH status (Fig. 4), it is interesting to note that an endoperoxide 1,2-dioxolane FINO₂ also has been reported to induce ferroptosis without decreasing intracellular GSH [24,25]. Different from MNPE, however, the endoperoxide moiety of FINO₂ does not generate singlet oxygen. Because the endoperoxide bond is highly reactive, FINO₂ directly binds to iron and disturbs its homeostasis. Other compounds with endoperoxide moiety, artemisinin and its derivatives, are Chinese anti-malarial drugs and enhance the sensitivity of cells to ferroptosis [26]. They cause an increase in the concentration of intracellular ferrous iron but have no effect on GSH content. Thus FINO₂ and artemisinin may induce ferroptosis by initiating a multifaceted mechanism. Compared to these compounds, however, singlet oxygen is released from MNPE during cultivation and appears to induce ferroptosis, suggesting that their mechanisms of action are substantially different.

Considering the fact that MNPE induces ferroptosis without mediating the depletion of GSH (Fig. 4), it is possible that singlet oxygen triggers the release of free iron and/or inactivates Gpx4 in cells. In support of this possibility, it has been reported that singlet oxygen is capable of irreversibly inactivating glutathione reductase, thioredoxin reductase, and Gpx in a cell-free system [27,28], although photosensitizers were employed in these studies. Selenocysteine, which plays catalytic roles in Gpx and thioredoxin reductase, is more sensitive to oxidation than Cys. However, a recent in-vivo study revealed that selenocysteine-containing wild-type Gpx4 is capable of conferring resistance to irreversible over-oxidation caused by peroxides [29]. Thus, the issues of how singlet oxygen affects iron status or Gpx4 activities remain unclear at present and further clarification is awaited.

In summary, evidence is provided for the first time, to show that singlet oxygen, which is generated from naphthalene endoperoxide in pure form, triggers ferroptosis in cultivated cells. Different from apoptosis, ferroptosis stimulates the release of intracellular biological molecules, which may be involved in aggravating inflammation or autoimmune responses under conditions of singlet

oxygen production. Naphthalene endoperoxides are clearly helpful for understanding singlet oxygen-mediated ferroptosis, which may contribute to therapeutics for singlet oxygen-involved pathogenesis.

Conflicts of interest

The authors declare no conflicts of interest.

Acknowledgments

This work was partly supported by the YU-COE [C31-3] program of Yamagata University.

Appendix A. Supplementary data

Supplementary data to this article can be found online at <https://doi.org/10.1016/j.bbrc.2019.08.073>.

References

- [1] S.J. Dixon, K.M. Lemberg, M.R. Lamprecht, R. Skouta, E.M. Zaitsev, C.E. Gleason, D.N. Patel, A.J. Bauer, A.M. Cantley, W.S. Yang, B. Morrison, B.R. Stockwell, Ferroptosis: an iron-dependent form of nonapoptotic cell death, *Cell* 149 (2012) 1060–1072, <https://doi.org/10.1016/j.cell.2012.03.042>.
- [2] J.P. Friedmann Angeli, M. Schneider, B. Proneth, Y.Y. Tyurina, V.A. Tyurin, V.J. Hammond, N. Herbach, M. Aichler, A. Walch, E. Eggenhofer, D. Basavarajappa, O. Rådmark, S. Kobayashi, T. Seibt, H. Beck, F. Neff, I. Esposito, R. Wanke, H. Förster, O. Yefremova, M. Heinrichmeyer, G.W. Bornkamm, E.K. Geissler, S.B. Thomas, B.R. Stockwell, V.B. O'Donnell, V.E. Kagan, J.A. Schick, M. Conrad, Inactivation of the ferroptosis regulator Gpx4 triggers acute renal failure in mice, *Nat. Cell Biol.* 16 (2014) 1180–1191, <https://doi.org/10.1038/ncb3064>.
- [3] W.S. Yang, R. SriRamaratnam, M.E. Welsch, K. Shimada, R. Skouta, V.S. Viswanathan, J.H. Cheah, P.A. Clemons, A.F. Shamji, C.B. Clish, L.M. Brown, A.W. Girotti, V.W. Cornish, S.L. Schreiber, B.R. Stockwell, Regulation of ferroptotic cancer cell death by GPX4, *Cell* 156 (2014) 317–331, <https://doi.org/10.1016/j.cell.2013.12.010>.
- [4] J. Krutmann, Ultraviolet A radiation-induced biological effects in human skin: relevance for photoaging and photodermatosis, *J. Dermatol. Sci.* 23 (Suppl 1) (2000) S22–S26, <http://www.ncbi.nlm.nih.gov/pubmed/10764987>.
- [5] L.O. Klotz, N.J. Holbrook, H. Sies, UVA and singlet oxygen as inducers of cutaneous signaling events, *Curr. Probl. Dermatol.* 29 (2001) 95–113, <http://www.ncbi.nlm.nih.gov/pubmed/11225205>.
- [6] R.M. Tyrrell, Solar ultraviolet A radiation: an oxidizing skin carcinogen that activates heme oxygenase-1, *Antioxidants Redox Signal.* 6 (2004) 835–840, <https://doi.org/10.1089/ars.2004.6.835>.
- [7] U. Chilakamarthi, L. Giribabu, Photodynamic therapy: past, present and future, *Chem. Rec.* 17 (2017) 775–802, <https://doi.org/10.1002/tcr.201600121>.

- [8] K. Otsu, K. Sato, Y. Ikeda, H. Imai, Y. Nakagawa, Y. Ohba, J. Fujii, An abortive apoptotic pathway induced by singlet oxygen is due to the suppression of caspase activation, *Biochem. J.* 389 (2005) 197–206, <https://doi.org/10.1042/BJ20042067>.
- [9] Y. Nagaoka, K. Otsu, F. Okada, K. Sato, Y. Ohba, N. Kotani, J. Fujii, Specific inactivation of cysteine protease-type cathepsin by singlet oxygen generated from naphthalene endoperoxides, *Biochem. Biophys. Res. Commun.* 331 (2005) 215–223, <https://doi.org/10.1016/j.bbrc.2005.03.146>.
- [10] D. Suto, K. Sato, Y. Ohba, T. Yoshimura, J. Fujii, Suppression of the pro-apoptotic function of cytochrome c by singlet oxygen via a haem redox state-independent mechanism, *Biochem. J.* 392 (2005) 399–406, <https://doi.org/10.1042/BJ20050580>.
- [11] D. Suto, Y. Iuchi, Y. Ikeda, K. Sato, Y. Ohba, J. Fujii, Inactivation of cysteine and serine proteases by singlet oxygen, *Arch. Biochem. Biophys.* 461 (2007) 151–158, <https://doi.org/10.1016/j.abb.2007.03.020>.
- [12] P. Di Mascio, G.R. Martinez, S. Miyamoto, G.E. Ronsein, M.H.G. Medeiros, J. Cadet, Singlet molecular oxygen reactions with nucleic acids, lipids, and proteins, *Chem. Rev.* 119 (2019) 2043–2086, <https://doi.org/10.1021/acs.chemrev.8b00554>.
- [13] J. Lee, E.S. Kang, S. Kobayashi, T. Homma, H. Sato, H.G. Seo, J. Fujii, The viability of primary hepatocytes is maintained under a low cysteine–glutathione redox state with a marked elevation in ophthalmic acid production, *Exp. Cell Res.* 361 (2017) 178–191, <https://doi.org/10.1016/j.yexcr.2017.10.017>.
- [14] T. Mukaide, Y. Hattori, N. Misawa, S. Funahashi, L. Jiang, T. Hirayama, H. Nagasawa, S. Toyokuni, Histological detection of catalytic ferrous iron with the selective turn-on fluorescent probe RhoNox-1 in a Fenton reaction-based rat renal carcinogenesis model, *Free Radic. Res.* 48 (2014) 990–995, <https://doi.org/10.3109/10715762.2014.898844>.
- [15] J.Y. Cao, S.J. Dixon, Mechanisms of ferroptosis, *Cell. Mol. Life Sci.* 73 (2016) 2195–2209, <https://doi.org/10.1007/s00018-016-2194-1>.
- [16] R. Itri, H.C. Junqueira, O. Mertins, M.S. Baptista, Membrane changes under oxidative stress: the impact of oxidized lipids, *Biophys. Rev.* 6 (2014) 47–61, <https://doi.org/10.1007/s12551-013-0128-9>.
- [17] D.J. Granville, C.M. Carthy, H. Jiang, G.C. Shore, B.M. McManus, D.W. Hunt, Rapid cytochrome c release, activation of caspases 3, 6, 7 and 8 followed by Bap31 cleavage in HeLa cells treated with photodynamic therapy, *FEBS Lett.* 437 (1998) 5, [https://doi.org/10.1016/S0014-5793\(98\)01193-4](https://doi.org/10.1016/S0014-5793(98)01193-4).
- [18] A. Valencia, J. Morán, Reactive oxygen species induce different cell death mechanisms in cultured neurons, *Free Radic. Biol. Med.* 36 (2004) 1112–1125, <https://doi.org/10.1016/j.freeradbiomed.2004.02.013>.
- [19] X. Ding, Q. Xu, F. Liu, P. Zhou, Y. Gu, J. Zeng, J. An, W. Dai, X. Li, Hematoporphyrin monomethyl ether photodynamic damage on HeLa cells by means of reactive oxygen species production and cytosolic free calcium concentration elevation, *Cancer Lett.* 216 (2004) 43–54, <https://doi.org/10.1016/j.canlet.2004.07.005>.
- [20] M.E. Wieder, D.C. Hone, M.J. Cook, M.M. Handsley, J. Gavrilovic, D.A. Russell, Intracellular photodynamic therapy with photosensitizer–nanoparticle conjugates: cancer therapy using a “Trojan horse”, *Photochem. Photobiol. Sci.* 5 (2006) 727–734, <https://doi.org/10.1039/b602830f>.
- [21] I. Saito, T. Matsuura, K. Inoue, Formation of superoxide ion from singlet oxygen. Use of a water-soluble singlet oxygen source, *J. Am. Chem. Soc.* 103 (1981) 188–190, <https://doi.org/10.1021/ja00391a035>.
- [22] A.W. Nieuwint, J.M. Aubry, F. Arwert, H. Kortbeek, S. Herzberg, H. Joenje, Inability of chemically generated singlet oxygen to break the DNA backbone, *Free Radic. Res. Commun.* 1 (1985) 1–9, <http://www.ncbi.nlm.nih.gov/pubmed/3880013>.
- [23] C. Pierlot, J.M. Aubry, K. Briviba, H. Sies, P. Di Mascio, Naphthalene endoperoxides as generators of singlet oxygen in biological media, *Methods Enzymol.* 319 (2000) 3–20, <http://www.ncbi.nlm.nih.gov/pubmed/10907494>.
- [24] R.P. Abrams, W.L. Carroll, K.A. Woerpel, Five-membered ring peroxide selectively initiates ferroptosis in cancer cells, *ACS Chem. Biol.* 11 (2016) 1305–1312, <https://doi.org/10.1021/acscchembio.5b00900>.
- [25] M.M. Gaschler, A.A. Andia, H. Liu, J.M. Csuka, B. Hurllocker, C.A. Vaiana, D.W. Heindel, D.S. Zuckerman, P.H. Bos, E. Reznik, L.F. Ye, Y.Y. Tyurina, A.J. Lin, M.S. Shchepinov, A.Y. Chan, E. Peguero-Pereira, M.A. Fomich, J.D. Daniels, A. V Bekish, V. V Shmanai, V.E. Kagan, L.K. Mahal, K.A. Woerpel, B.R. Stockwell, FINO2 initiates ferroptosis through GPX4 inactivation and iron oxidation, *Nat. Chem. Biol.* 14 (2018) 507–515, <https://doi.org/10.1038/s41589-018-0031-6>.
- [26] G.-Q. Chen, F.A. Benthani, J. Wu, D. Liang, Z.-X. Bian, X. Jiang, Artemisinin compounds sensitize cancer cells to ferroptosis by regulating iron homeostasis, *Cell Death Differ.* (2019), <https://doi.org/10.1038/s41418-019-0352-3>.
- [27] T. Tabatabaie, R.A. Floyd, Susceptibility of glutathione peroxidase and glutathione reductase to oxidative damage and the protective effect of spin trapping agents, *Arch. Biochem. Biophys.* 314 (1994) 112–119, <https://doi.org/10.1006/abbi.1994.1418>.
- [28] A. Suryo Rahmanto, D.I. Pattison, M.J. Davies, Photo-oxidation-induced inactivation of the selenium-containing protective enzymes thioredoxin reductase and glutathione peroxidase, *Free Radic. Biol. Med.* 53 (2012) 1308–1316, <https://doi.org/10.1016/j.freeradbiomed.2012.07.016>.
- [29] I. Ingold, C. Berndt, S. Schmitt, S. Doll, G. Poschmann, K. Buday, A. Roveri, X. Peng, F. Porto Freitas, T. Seibt, L. Mehr, M. Aichler, A. Walch, D. Lamp, M. Jastroch, S. Miyamoto, W. Wurst, F. Ursini, E.S.J. Arnér, N. Fradejas-Villar, U. Schweizer, H. Zischka, J.P. Friedmann Angeli, M. Conrad, Selenium utilization by GPX4 is required to prevent hydroperoxide-induced ferroptosis, *Cell* 172 (2018) 409–422, <https://doi.org/10.1016/j.cell.2017.11.048>, e21.